

Measuring infiltration rate and hydraulic conductivity in a dry well in a thin overburden

Kobra Sheikh Leiveci^{1*}, Gholam Abbas Kazemi¹, Noorali Damough²

¹ Faculty of Earth Sciences, University of Shahrood, Shahrood, Iran

² Khuzestan Water and Power Authority, Ahvaz, Iran

*Corresponding author, e-mail: k.sh82@yahoo.com

(received: 28/11/2015 ; accepted: 04/05/2016)

Abstract

Infiltration rate and hydraulic conductivity are immensely important parameters for evaluating the hydrology of subsurface environments. Specifically, in disposal wells schemes and in artificial recharge plans both properties must be correctly assessed to better analyze the performance of these installations. In a new research, tanker water and rainfall runoff were injected into a 22.5 m deep well dug in a 15 m thick dry overburden and the underlying impermeable marl bedrock (7.5 m) to evaluate the feasibility of using the well to store winter runoff in the overburden for recovery in the summer. Rates of rise and fall in the hydraulic head were measured, and infiltration rate in various depths were calculated. Also, hydraulic conductivity of the overburden was calculated using particle distribution curves of the overburden samples. Infiltration rate showed close correlation with the hydraulic conductivity. Maximum infiltration rate occurs at depths of 10-11 m; depth of 10 m is the most conductive interval. New findings have come out of this experience including 1. negative correlation between maximum head generated in a specific injection event and the rate of infiltration and 2. the important role of the contact zone between bedrock and the overburden in draining the injected water.

Keywords: Hydraulic Conductivity, Infiltration Rate, Recharge Well, Soil Grain Size, Water Injection.

Introduction

Infiltration rate and hydraulic conductivity are immensely important parameters for accurately evaluating the hydrology and groundwater potential of subsurface environments. These two parameters are very closely linked; the rate of infiltration is affected greatly by the hydraulic conductivity of the sediments. Infiltration rate is usually determined from field data. Different techniques and various types of instruments have been used for measuring infiltration rate, but the principal methods are flooding of basins or furrows, sprinkling, double or single-ring infiltrometers, and inversed auger hole (Diamond & Shanley, 1998; Van Hoorn, 1979).

One of the methods which is occasionally used to measure the infiltration rate in specific cases is the dry well technique. Dry wells are also used for some other purposes. These wells usually function as infiltration systems to reduce the quantity of runoff from a site, and recharge groundwater. Dry wells also treat storm water runoff through soil infiltration, adsorption, trapping, filtering, and bacterial degradation. However, these wells should only be used to infiltrate relatively clean runoff such as rooftop runoff (DEP, 2004; Cahill *et al.*, 2006). Most of the dry wells receive water directly from roof drain ladders or by storm drain inlets located in driveways or small parking lots. Some also have grated covers and receive surface runoff

from the surrounding lawn or paved areas.

One example of studies related to dry well is that by USEPA (2013). In this study, fifteen dry wells were monitored for water levels during periods ranging from two months to one year, or by controlled tests using municipal water from fire hydrants (EPA, 2013). The primary objective of the EPA study was to investigate the effectiveness of the Township of Millburn's use of on-site dry wells to limit storm water flows into the local drainage system. Hence, infiltration rate was calculated in each well using changes in water levels and Horton equation. In another study, Massmann (2004) used a special technique for estimating infiltration rates for dry wells that are constructed using standard configurations developed by the Washington State Department of Transportation.

Hydraulic conductivity is a significant parameter describing the ease with which flow takes place through a porous medium (Schwartz & Zhang, 2003). The experiments have shown that hydraulic conductivity depends on both properties of the porous medium and the fluid (Ishaku *et al.*, 2011). There are various factors that influence the hydraulic conductivity of a soil; the viscosity of the fluid flowing through the soil, the size, shape, and amount of soil particles and void spaces, and the degree of saturation of the soil. Many techniques for the determination of hydraulic conductivity

under laboratory or field conditions have been described in Freeze and Cherry (1979) and Todd and Mays (2005).

Hydraulic conductivity is divided into saturated and unsaturated hydraulic conductivity; saturated hydraulic conductivity being the most commonly measured one. Methods used to determine the saturated hydraulic conductivity of soil include laboratory methods such as the constant head test and the falling head test and field methods including among others pumping tests, slug tests, and injection tests (Ren & Yan, 2014; Philips & Kitch, 2005).

The cost of field operations and associated wells constructions can be prohibitive as well, but there is a more simple method which is referred to as grain-size analysis. Empirical formulae based on grain-size distribution characteristics have been developed and used to overcome the problem (Odong, 2007). For example, Kozeny (1927) offered a formula which was then modified by Carman (1937, 1956) to become the Kozeny-Carman equation. Other attempts were made by Hazen (1892), Terzaghi and Peck (1964) and more recently Alyamani and Sen (1993). The applicability of each of these formulae depends on the type of soil for which hydraulic conductivity is to be calculated.

In the present study, we have measured both hydraulic conductivity and infiltration rate in a dry well. Hydraulic conductivity has been calculated using empirical formula and infiltration rate was measured by monitoring hydraulic head in the studied well. The difference between this research and its predecessors is the geometrical setting of the studied dry well. The studied well has been hand dug in a dry thin overburden which is underlain by thick impermeable marl bedrock. The overburden is 15 m in thickness and the total depth of the well is 22.5 m.

In all published cases, dry wells do not penetrate into bedrock and are completed in the unsaturated zone only. Therefore, the configuration of the studied well in this research differs from the previous studies. It should also be added that these types of research through which water is repeatedly injected into dry formations have seldom been practiced because of the high costs involved. However, as it can be seen in the following sections, the results obtained are also quite novel and worth spending considerable amount of budget.

Specifications of the study well

The study well is a test dry well with the geographical coordinates of 31° 33' 31.33" north latitude and 49° 23' 15.3" east longitude, located 4 km to the east of Gazin village and 14 km to the northwest of Haftkel in Khuzestan province, southwest Iran (Fig. 1). The well in question has been hand dug to the depth of 22.5 meters. It is 1.20 m in diameter to the depth of 10 meters gradually reducing to 90 cm below that. The geology in the well, from land surface to the depth of 15 meters is overburden deposits; from depth of 16 to 22.5 meters it consists of Mishan formation which is gray impermeable marl. It should be pointed out that it was easy and quick to dig the overburden part of the well by hand. In contrast, the formation part (compact apparently drained marl) was extremely difficult to dig even using gas compressor.

The study dry well is located inside a one-acre chicken farm facility. It was dug to produce groundwater (if any) for the mentioned chicken farm but it turned out to be dry. After failure of the well, an idea was developed to use this well to create a short lived artificial aquifer as an accommodation to store winter runoff for immediate subsequent recovery in the following summer. The intended runoff originates from the chicken farm's roof and yard and also from the nearby upslope terrain. A simple filter was built to trap fine sediments from winter run off before injection to avoid clogging of the well.

Materials and Methods

Measurement of infiltration rate

To calculate the infiltration rate, 9 injection events were carried out from 2011 to 2014. Of these, 6 events were undertaken using runoff as the source of injecting water. In 2013 and early 2014, occurrence of rainfall in the study area was timely and above mean annual average. This led to the well growth of short rooted crops resulting in good vegetation cover. As a consequence, not enough runoff was generated. Clean municipal water was therefore injected into the well in 3 injection events. Specifications of all 9 injections are displayed in Table 1. In all events, infiltration rate at various depths was calculated by measuring changes in hydraulic head in the well.

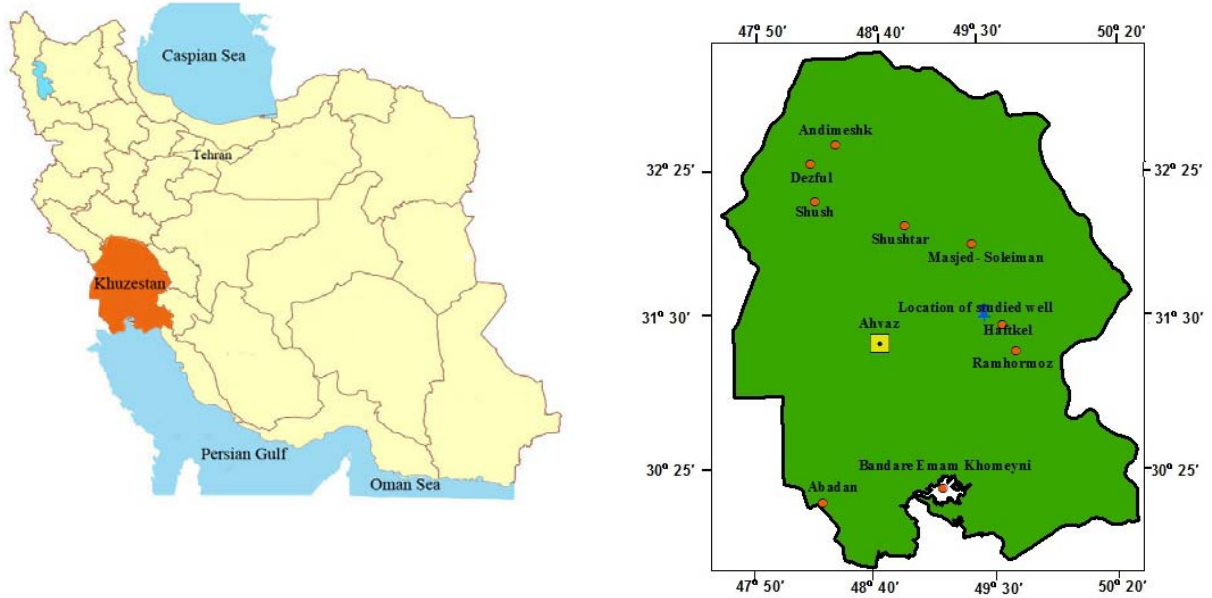


Figure 1. Location of the study area in northwest of Haftkel, Khuzestan

Table 1. Characteristics of injection events

Event	Date of injection	Duration of injection (min)	Injection rate (m3/hr)	Volume of water injected (m ³)
1	21/1/2012	120	15	30
2	24/11/2012	840	3.5	49
3	8/12/2012	300	3.5	17.5
4	11/12/2012	480	3.5	28
5	21/12/2012	300	3.5	17.5
6	26/12/2012	120	3.5	7
7	26/3/2014	50	20.4	17
8	26/3/2014	17	60	17
9	14/4/2014	37	27.5	17

The infiltration rate changes depending on the time after injection and the elevation of hydraulic head (Table 2). Figures 2 to 5 display infiltration curves for various injection events. A schematic diagram illustrating how water infiltrates into the overburden after injection is displayed in Figure 6. It should be noted that in all injection events, the injected water remains in the bottom of the well (lower part of the Marl of Mishan formation) for a very long time and never dries out. This shows that evaporation is not a significant process inside the well. If evaporation was an effective process, the well should have turned dry sometime after injection but the well always contains some water

which neither evaporates nor infiltrates.

Dry and wet sieving of overburden samples

In order to measure particle size and hydraulic conductivity of the slope washed materials in the studied well, 15 soil samples were taken from different depths of the study well using lifts.

Collected samples are from depths 1 to 15 meters, each meter one sample, and have been subjected to dry and wet sieve analysis. Of the two methods, wet sieving is seldom practiced; it is therefore discussed in more detail in the following lines. Figures 7 and 8 show particle size distribution curves for the collected samples.

Table 2. Change in hydraulic head and infiltration rate in all injections

Event	Time (min)	Hydraulic Head (m)	Infiltration rate (cm/h)	Event	Time (min)	Hydraulic Head (m)	Infiltration rate (cm/h)	Event	Time (min)	Hydraulic Head (m)	Infiltration rate (cm/h)
1	0	16	0	7	0	11.8	0	9	0	11.7	0
	720	11	41.67		3	11.3	1000		1	11.6	600
	1227	7.8	37.87		6	10.7	1200		2	11.5	600
	1767	6.3	16.67		9	10.3	800		3	11.38	720
2	0	16.5	0		12	10.1	400		5	11.1	840
	1440	14	10.41		15	9.7	800		7	10.8	900
	2880	13.4	2.50		18	9.45	500		9	10.6	600
	4320	13.1	1.25		21	9.4	100		11	10.4	600
	5760	12.7	1.66		24	9.25	300		13	10.3	300
	7230	12.2	2.04		27	9.15	200		15	10.15	450
	9420	11.5	1.92		30	9.02	260		18	9.95	400
	12360	11.2	0.61		33	9	40		21	9.75	400
15900	9.9	2.20	38		8.9	120	24		9.6	300	
3	0	12	0		43	8.7	240		27	9.45	300
	1350	11.7	1.33		48	8.65	60		30	9.35	200
	2760	11.5	0.85		53	8.5	180		35	9.2	180
4	0	17.5	0	60	8.3	171	40	9.07	156		
	1650	17.1	1.45	70	8.2	60	45	8.9	204		
	2970	16.6	2.27	75	8	240	50	8.83	84		
	4380	16.4	0.85	0	12.6	0	55	8.75	96		
5	0	18.6	0	1	12.4	1200	60	8.65	120		
	1990	18.3	0.90	3	11.9	1500	65	8.55	120		
	2980	17.95	2.12	5	11.7	600	75	8.5	30		
6	0	19.2	0	7	11.3	1200	80	8.45	60		
	2680	17.9	2.92	10	11.1	400	90	8.35	60		
	5290	17.3	1.37	12	10.95	450	100	8.32	18		
	9310	15.7	2.39	14	10.78	510	110	8.25	42		
	14530	14.6	1.26	16	10.92	390	130	8.16	27		
	21820	11	2.96	18	10.55	300	140	8.12	24		
	24850	6	9.90	21	10.3	500	150	8.1	12		
	30310	4.9	1.20	24	10.1	400	160	8.08	12		
			27	10	200	180	8.02	18			
			30	9.9	240	200	7.97	15			
			35	9.7	240	220	7.93	12			
			40	9.5	214	280	7.8	13			
			47	9.25	126	347	7.7	8.95			
			57	9.04	126	438	7.65	3.30			
			67	8.85	114	498	7.59	6			
			77	8.71	84	558	7.52	7			
			87	8.6	66	633	7.48	3.2			
			97	8.5	60	687	7.44	4.44			
			107	11.8	42	1812	6.49	5.07			
			547	11.3	7.5	3371	6.09	1.54			
			832	10.7	6.32	4864	5.96	0.53			
			967	7.1	4.44	6317	16.67	0.53			
			1167	6.8	9	7707	16.76	0.39			
			1507	6.53	4.76	9028	16.82	0.27			
			2317	6.18	2.59	10600	16.88	0.23			
			2797	6.08	1.27	12018	16.95	0.30			
			3262	6.02	0.77	17085	17.02	0.08			
			3812	5.99	0.33	19061	17.04	0.06			
			4387	5.96	0.31	22144	17.08	0.07			
			4597	5.95	0.29	30815	17.2	0.08			
			5907	5.85	0.46	32034	17.21	0.05			
			6967	5.82	0.17	56176	17.44	0.06			
			7957	5.79	0.18						
			9457	5.75	0.16						
			9927	5.72	0.38						

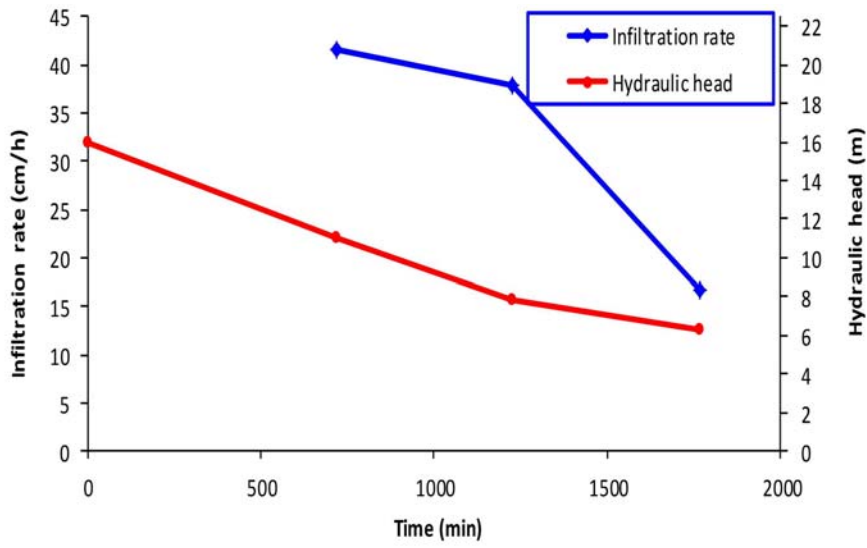


Figure 2. Change in infiltration rate with hydraulic head in first injection

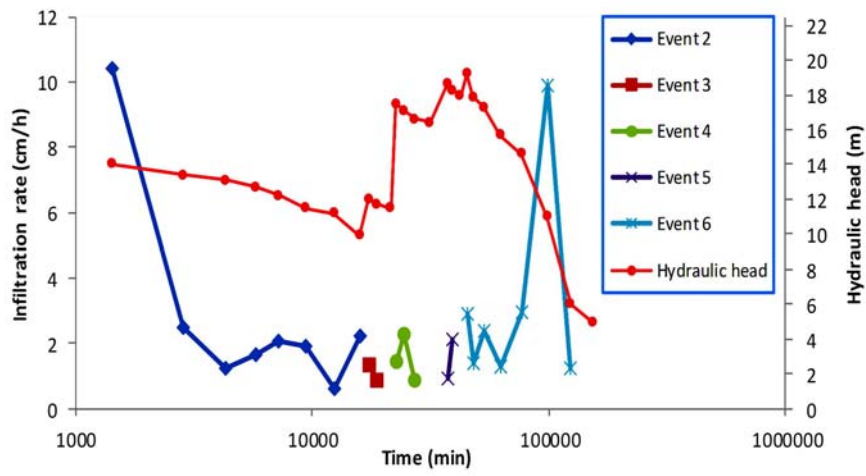


Figure 3. Change in infiltration rate with hydraulic head in second to sixth injections

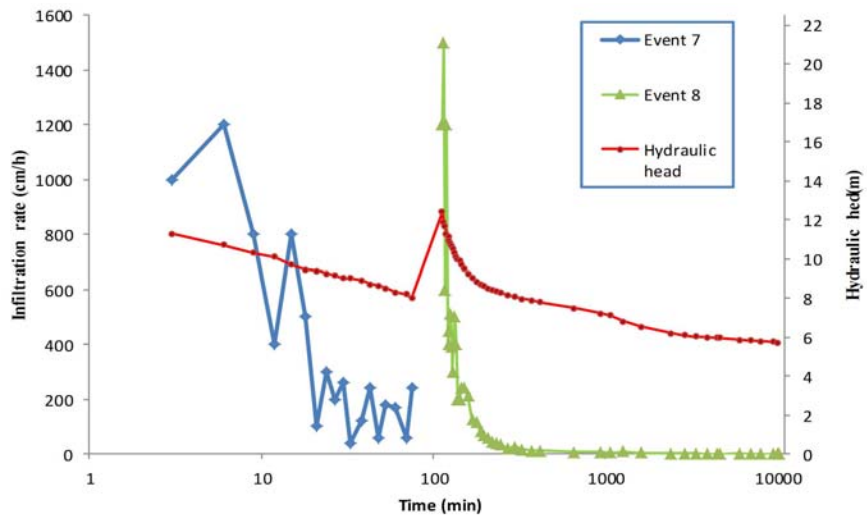


Figure 4. Change in infiltration rate with hydraulic head in seventh and eighth injections

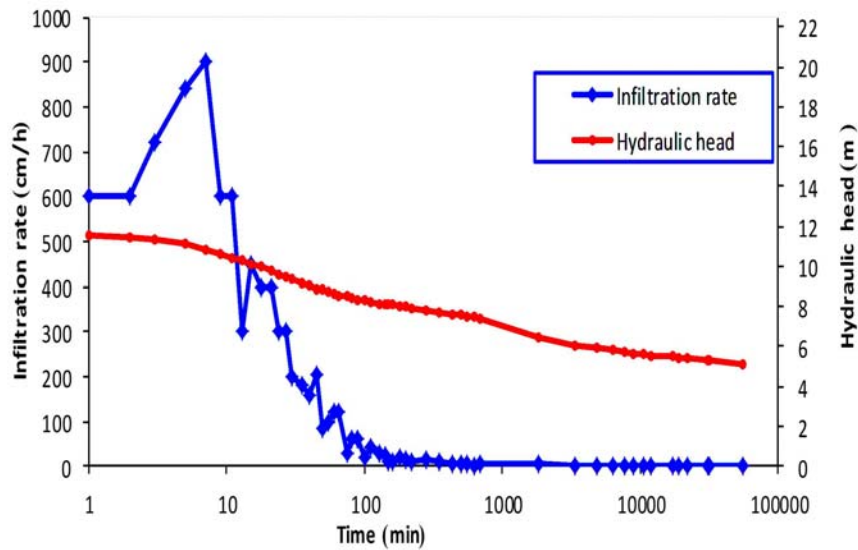


Figure 5 Change in infiltration rate with hydraulic head in ninth injection

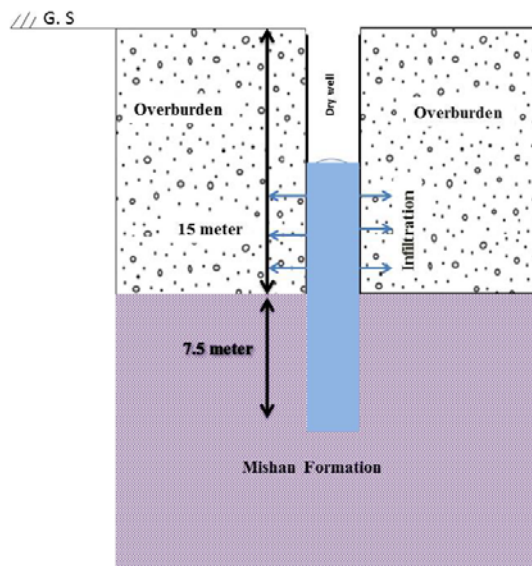


Figure 6. Infiltration of injected water into the overburden through the wall of the well

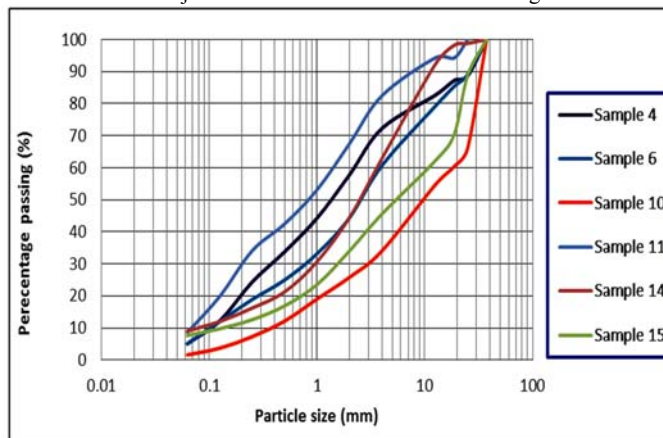


Figure 7. Size distribution curves of coarse particles through dry sieve

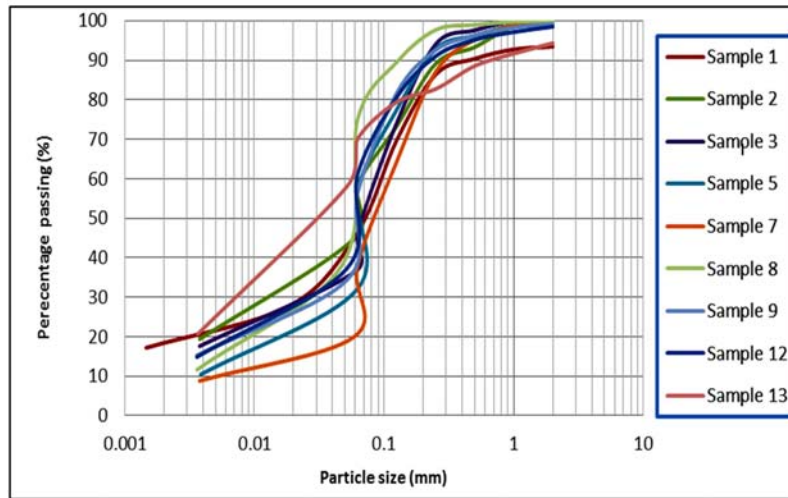


Figure 8. Size distribution curves of fine particles through wet sieve

Dry sieving is only applicable for clean granular materials. To be eligible for dry sieving, the soils in question should be sufficiently dry. For dry sieving, a specified amount of the sample is shaken for 10 minutes through various sizes of 5 mesh, 10 mesh, 18 mesh, 35 mesh, 60 mesh, 120 mesh, 230 mesh, and finally the pan. The percentage of the soil passing through each sieve is calculated using equation 1. Depending on the percentage of gravel, sand, and mud, the soil texture is determined by Folk classification triangle (Fig. 9).

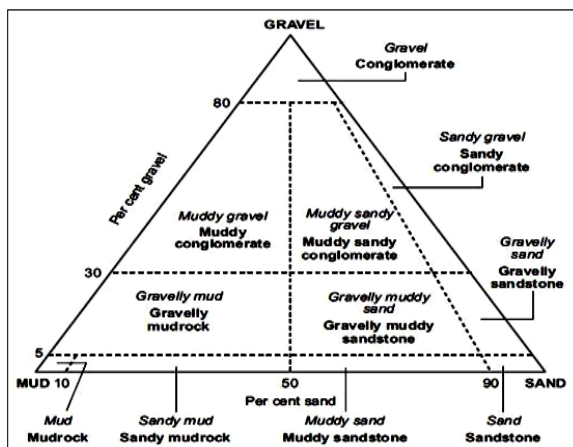


Figure 9 Folk triangle classification of sediments and clastic rocks based on particle sizes (adapted from Mousavi Harami 1996)

If soil sample is wet or damp, it should first be dried in the oven at a temperature not exceeding 110°C. The sample is then left in an open space to cool down before sieving. When wet fine grain samples loose moisture, their clay and silt particles

adhere together and form flocculation. Therefore, wet sieving is preferred for analyzing wet samples which contain a large amount of silt and clay. In wet sieving, soil samples are washed to ensure that the fine grains are separated from the coarse grains. The procedure is as follow:

1. The oven dried sample is weighted.
2. The sample is then put on sieve 230 mesh and is washed by water.
3. After washing, the sample is again dried in the oven for 4 hours.
4. The dried sample is then sieved in the same manner as the dry sieving.

The particle size distribution curves for all fine grain samples prepared by adopting Equation 1 are shown in Figure 9.

$$\% \text{ Passing} = 100 - \text{Percent retained on sieve} \quad (1)$$

$$\text{Percent retained on sieve} = \left(\frac{W_C}{W_T} \right) \times 100$$

where W_T is the total mass of sample and W_C is the cumulative weight retained on each sieve.

Estimation of hydraulic conductivity using particle size distribution curves

Hydraulic conductivity (K) can be calculated by particle size analysis of the soil samples of interest, using empirical equations relating K to some size property of the sediments. Vukovic and Soro (1992) abbreviated several empirical methods from former studies and presented a general formula as follow:

$$K = \frac{g}{\nu} \cdot c \cdot f(n) \cdot d_e^2 \quad (2)$$

where K is hydraulic conductivity, g is acceleration of gravity, ν is kinematic viscosity of water, C is sorting coefficient, f(n) is porosity function, and d_e is effective grain diameter that can be obtained from the curves of samples cumulative weight. The

kinematic viscosity (ν) is related to the dynamic viscosity (μ) and the fluid (water) density (ρ) as defined by:

$$\nu = \frac{\mu}{\rho} \quad (3)$$

The values of C , $f(n)$, and d_e depend on the different methods used in the grain-size analysis.

According to Vukovic and Soro (1992), porosity (n) may be derived from the empirical relationship with the coefficient of grain uniformity (U) as follows:

$$n = 0.255(1 + 0.83^U) \quad (4)$$

where U is the coefficient of grain uniformity and is given by:

$$U = \left(\frac{d_{60}}{d_{10}} \right) \quad (5)$$

Here, d_{60} and d_{10} represent the grain diameter in (mm) for which, 60% and 10% of the sample, respectively, are smaller. Former studies have presented equation 6 which takes the general form presented in Eq. (3) above but with varying C , $f(n)$, and d_e values and their domains of applicability.

Kozeny-Carman:

$$K = \frac{g}{\nu} \times 8.3 \times 10^{-3} \times \left[\frac{n^3}{(1-n)^2} \right] \quad (6)$$

The Kozeny-Carman equation is one of the most widely accepted and used derivations of

permeability as a function of the characteristics of the soil medium (Odong, 2007). This equation was originally proposed by Kozeny (1927) and was then modified by Carman (1937, 1956) to become the Kozeny-Carman equation. It is not appropriate for either soil with effective size above 3 mm or for clayey soils (Carrier, 2003). This method does not consider porosity and, therefore, porosity function takes on value 1. Breyer's formula is often considered most useful for heterogeneous materials and poorly sorted grains with uniformity coefficient between 1 and 20, and effective grain size between 0.06 mm and 0.6 mm.

Slitcher:

$$K = \frac{g}{\nu} \times 1 \times 10^{-2} \times n^{3.287} \times d_{10}^2 \quad (7)$$

This formula is most applicable for grain-size between 0.01 mm and 5 mm.

USDA:

$$K = 0.36 \times d_{20}^{2.3} \quad (8)$$

In this study, hydraulic conductivity (K) has been estimated based on the sieve analysis using the U.S Department of Agriculture formula (Weight and Sonderegger, 2001). Hydraulic conductivity values and other parameters required to calculate the empirical formula are presented in Table 3.

Table 3. Estimation of hydraulic conductivity of the soil samples (The number of sample represents the depth of sampling)

Sample & its classification	d_{10}	d_{20}	d_{30}	d_{50}	d_{60}	U	n	Slitcher (m/day)	Kazni-Karman (m/day)	USDA (m/day)
1. Muddy sand	---	0.004	0.0246	0.741	0.1	---	---	---	---	0.0001
2. Muddy sand	---	0.004	0.012	0.06	0.064	---	---	---	---	0.0001
3. Muddy sand	---	0.006	0.0287	0.071	0.09	---	---	---	---	0.0002
4. Sandy gravel	0.1	0.2	0.39	1.36	2.15	21.50	0.26	1	2.22	0.77
5. Muddy sand	0.0037	0.0155	0.046	0.06	0.07	18.92	0.26	0.001	0.003	0.0021
6. Sandy gravel	0.1	0.3	0.8	2.51	4	40	0.26	0.94	2.08	1.95
7. Muddy sand	0.006	0.0518	0.0644	0.08	0.125	20.83	0.26	0.004	0.008	0.0343
8. Muddy sand	0.003	0.01	0.0316	0.0066	0.067	21.93	0.26	0.001	0.002	0.0008
9. Gravelly sand	---	0.007	0.0373	0.06	0.07	---	---	---	---	0.0003
10. Sandy gravel	0.334	1	3	10	17.3	51.80	0.26	10.47	23.18	31.10
11. Muddy sandy gravel	0.133	0.24	0.4	1.73	2.68	20.15	0.26	6.49	4	1.79
12. Muddy sand	---	0.0079	0.03	0.071	0.089	---	---	---	---	0.0005
13. Gravelly mud	---	0.0033	0.0072	0.0334	0.06	---	---	---	---	0.0001
14. Sandy gravel	0.07	0.4	0.9	2.72	3.67	52.43	0.26	0.72	3.14	0.49
15. Sandy gravel	0.11	0.7	1.49	5.48	11.05	100.45	0.26	0.46	139.46	3.78

Results and Discussion

Up until now, a known fact was that infiltration rate decreases with passing time until it reaches a nearly constant rate which is generally referred to as “base infiltration”. However, in this study, infiltration rate in some injection events increases as time goes by, something that is difficult to justify. In second injection, re-increase in the infiltration rate happens at depths of 4 to 11.5 m and 11.3 to 12.6 m. In the 6th injection, re-increase happens at depths of 2.5-6.8 m and 7.9-16.5 m. In the other injection events, a more or less similar situation is noted. These abnormal increases appear as peaks in the infiltration curves which is seen in Figures 3-5. It is likely that uneven effective radius of the well in different depths is responsible for this abnormality.

In different depths of the study well, the infiltrated water moves away from the well point to a particular distance depending on the hydraulic conductivity of the depth in question. The infiltrated water then returns back into the well compartment if water level in the well point falls below the specific depth. Rapid decline in water level in the well compared to the slow velocity of horizontal movement of the water moving away from the well causes infiltrated water to return back. The returned infiltrated water moves vertically downward and re-infiltrates into the lower horizons of the formation. The cycle of infiltration into upper horizons, returning of infiltrated water back into the well compartment, vertical movement (fall), and re-infiltration into the lower horizons of the formation causes fluctuation in the calculated infiltration rate as displayed in Figures 3-5.

Maximum values of infiltration rate have been noted for injection events 7, 8, and 9, amounting to 371, 201, and 158 cm/h, respectively. Among all injection events, maximum infiltration rate occurs in the 7th injection event, probably due to 17 months lag time with the previous injection and the resultant saturation deficit created by this long delay. In events 1 to 6, for which runoff was used as the injectant, infiltration rate showed less fluctuation and was lower than events 7 to 9 through which tanker water was injected. It is likely that clogging by sands and clays present in the runoff is the cause of lower infiltration rate in events 1-6.

This study has shown that the average infiltration rate depends on the total head generated during injection; there is a negative correlation between

maximum head generated and the rate of infiltration (Fig. 10).

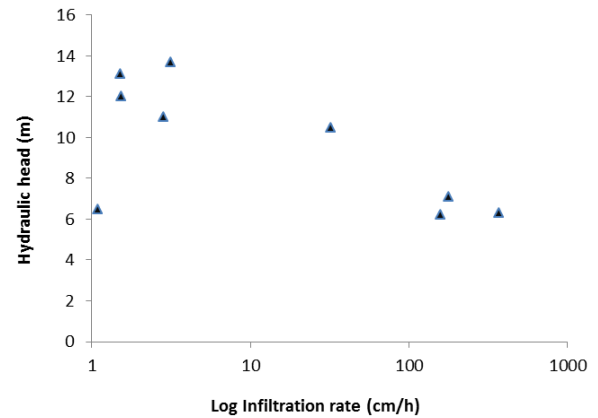


Figure 10. The relationship between maximum hydraulic head generated in each injection event and the infiltration rate

Three explanations can be provided for this apparently abnormal situation. Firstly, higher hydraulic heads can lead to the compaction of the overburden in the well face with consequent clogging of the openings. Secondly, higher hydraulic heads may result in flow turbulence causing reduction in the flow rate. Thirdly, tanker water contains less fine particles compared to runoff and consequently can bring about higher infiltration rate.

Calculations have shown that the majority of water infiltrates into depths 10 and 11 m. It should be pointed out that the depth of 16 meters comprises partly of marls belonging to Mishan formation which is impermeable. Because of the existence of the erosional surface between the overburden and the Mishan formation, the contact zone of the two is a highly conductive zone. If this conductive zone did not exist, drop in the hydraulic head below overburden was not expectable.

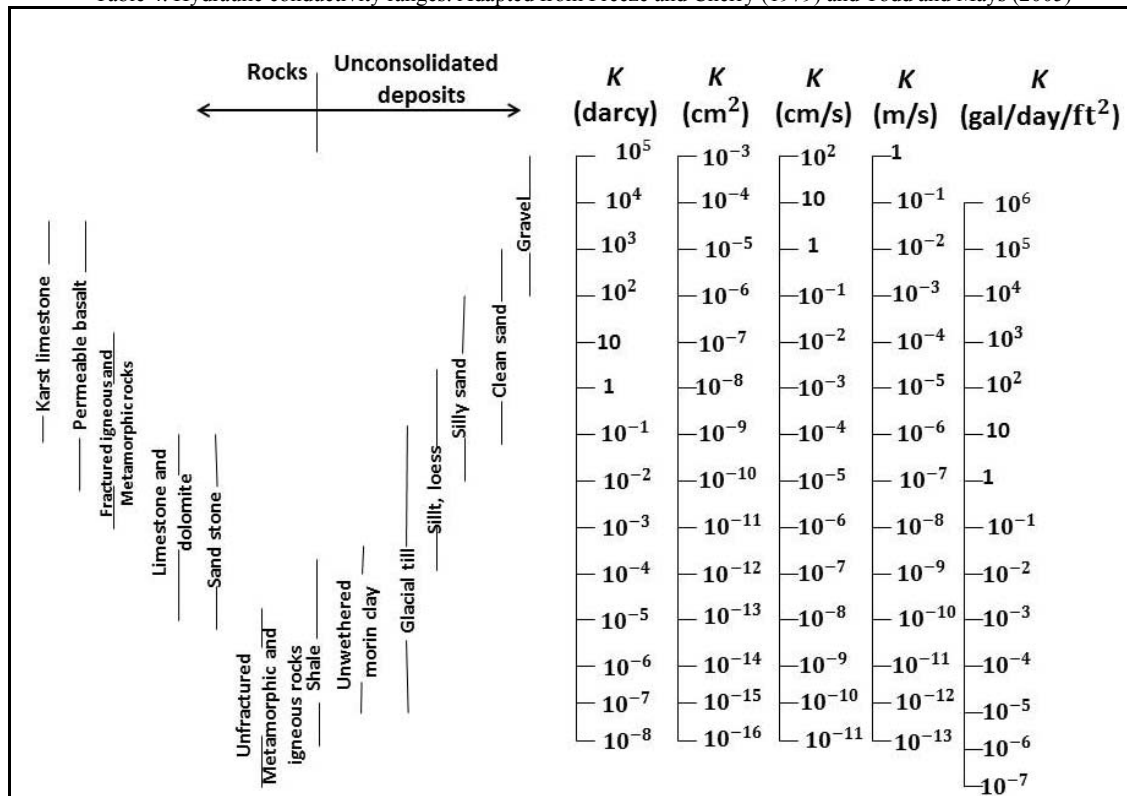
Due to large fluctuation in the infiltration rate, hydraulic conductivity is needed to be investigated to increase the validity of infiltration rate estimates. The infiltration rate would not correspond, even under ideal field conditions, with the hydraulic conductivity as normally determined in the laboratory. That is, the standard laboratory (K) equals the infiltration rate only when the sediments are saturated. Table 3 shows that the hydraulic conductivities calculated by Slitcher's method are in all cases lower than values estimated by the other methods, which is consistent with the conclusion by Vukovic and Soro (1992), Cheng and Chen (2007),

Odong (2007), and Heidari (2011). Therefore, the figures estimated by USDA method for samples 1, 2, 3, 9, 12, and 13 are higher than other formulas and possibly the best estimations for this study.

Like infiltration rate, the hydraulic conductivity was calculated for different depths of the overburden. Calculated hydraulic conductivity values have been compared to values for different soils reported by Todd and Mays (2005), McWhorter (1977), and Freeze and Cherry (1979). The values are within the same ranges which prove

the accuracy of our tests (Table 4). As it can be seen from Figure 8, Sample 11 is finer than the other samples but its hydraulic conductivity is higher than Sample 4 which is a coarse grain one. High hydraulic conductivity at depth 11 m is possibly due to the existence of more sand in this interval. Samples collected from depth 1 to 9 m are fine grain and exhibit muddy sand texture. The exception is depths 4 and 6 m which are coarse grain.

Table 4. Hydraulic conductivity ranges. Adapted from Freeze and Cherry (1979) and Todd and Mays (2005)



Conclusions

In this research, runoff water and tanker water were injected into a 22.5 m deep dry well in 9 different occasions. In addition, soil samples collected from different depths in the studied well were subjected to grain size analysis. The rate of infiltration exhibited significant variations in different injection events; hydraulic conductivity calculated through several empirical formulas also showed large differences. Soil type is the main factor controlling the hydraulic conductivity. Depth 10 meter is the most conductive interval because it is coarse grain and contains gravel. Similarly, infiltration rate is greatest in depths 10-11 m.

This study has shown that infiltration rate and

hydraulic conductivity values show close correlation and both are essential for estimating the volume of water that can be recharged and recovered in any subsurface environment. It has been found that the USDA formula is the most suitable for calculating hydraulic conductivity; the hydraulic conductivity estimated by the Slitcher's formula is lower than the other methods. Although depths lower than 16 m include impermeable grey marl, drop in the hydraulic head was recorded up to depth 17 m in all injection events below which the infiltration ceases. It is therefore concluded that the contact zone binding overburden to the underlying grey marl is hydraulically permeable and the injected water escapes through this zone.

References

- Cahill, M., Derek, C., Sowles, M., 2011. Dry wells. Oregon State University, From Oregon Sea Grant, Corvallis, 8 pp.
- Carman, P.C., 1937. Fluid flow through granular beds. *Trans. Inst. Chem. Eng.* 15:150 pp.
- Carman, P.C., 1956. Flow of gases through porous media. Butterworths scientific publications, London 6-12.
- Carrier, W.D., 2003. Goodbye, Hazen; hello, Kozeny-Carman. *ASCE Journal of Geotech Geoenviron Eng.* 129 (11): 1054–1056.
- Cheng, C., Chen, X.H., 2007. Evaluation of methods for determination of hydraulic properties in an aquifer-aquitard system hydro logically connected to river. *Hydrogeol Journal* 15: 669–678.
- Connecticut Department of Environmental Protection, 2004. Connecticut Storm water Quality Manual. <http://dep.state.ct.us>
- Diamond, J., Shanley, T., 1998. Infiltration rate assessment of some major soils. End of Project Report, Armis 4102, Teagasc, Dublin.
- Environmental Protection Agency, 2013. Evaluation of dry wells and cisterns for storm water control: Millburn Township, NJ. EPA 600/R-12/600.
- Freeze, R.A., Cherry, J.A., 1979. Groundwater. Prentice Hall, Englewood Cliffs, NJ, 604 pp.
- Hazen, A., 1892. Some physical properties of sands and gravels. Massachusetts State Board of Health, 24th annual report, Boston, pp 539–556.
- Heidari, M.M., 2011. Determination of permeability coefficient based on distribution curve. Third national conference on irrigation and drainage network, Ahvaz, March 1-3, 2011.
- Ishaku, J.M., Gadzama, E.W., Kaigama, U., 2011. Evaluation of empirical formulae for the determination of hydraulic conductivity based on grain-size analysis. *Journal of Geology and Mining Res* 3(4): 105–113.
- Johnson, A.I., 1963. A field method for measurement of infiltration. U. S, Geological Survey Water Supply Paper 1544–F.
- Kozeny, J., 1927. Uber kapillare leitung des wassers in boden: Sitzungsber [On capillary flow of water in soil], Sitz Ber Akad Wiss Wien, Vienna, 136: 271–306.
- Massmann, J., 2004. An approach for estimating infiltration rates for storm water infiltration dry wells. Washington State Department of Transportation Technical Monitor, 68 pp.
- Mousavi Harami, A., 2007. Sedimentology. 8th edition, Razavi Ghods Astan, Mashhad, 474 pp. (In Persian).
- McWhorter, D.B., Sunada, D.K., 1977. Groundwater Hydrology and Hydraulics. Water Resources Publications, Fort Collins, CO, 290 pp.
- Odong, J., 2007. Evaluation of empirical formulae for determination of hydraulic conductivity based on grain-size analysis. *Journal Am Sci.* 3(3): 54–60.
- Philips, C.E., Kitch, W.A., 2011. A review of methods for characterization of site infiltration with design recommendations. In: Proceedings of 43rd Symposium on Engineering Geology and Geotechnical Engineering, Las Vegas, Nevada.
- Ren, Lu., Yan, Xu., 2014. The streambed sediment grain size analysis and empirical formula of vertical hydraulic conductivity of Wei River. *Journal of Applied Sciences and Engineering Research.* 3(2): 411–421.
- Schwartz, F.W., Zhang, H., 2003. Fundamentals of Groundwater, John Wiley & Sons, 583 pp.
- Steiakakis, E., Gamvroudis, C., Alevizos, G., 2012. Kozeny-Carman equation and hydraulic conductivity of compacted clayey soils, *Geomaterials* 2: 37–41.
- Terzaghi, K., Peck, R.B., 1964. Soil Mechanics in Engineering Practice. Wiley, New York.
- Todd, D.K., Mays, L.W., 2005. Groundwater Hydrology, Wiley, Hoboken, NJ, 636 pp.
- Van Hoorn, J.W., 1979. Determining hydraulic conductivity with the inversed auger hole and infiltrometer methods. In: Wesseling, J. (ed.), Proceedings of the International Drainage Workshop, ILRI Publication 25, Wageningen, The Netherlands, ILRI, pp. 150–154.
- Vukovic, M., Soro, A., 1992. Determination of hydraulic conductivity of porous media from grain-size composition. Water Resources Publications, Littleton, Colorado, 83 pp
- Weight, W.D., Sonderegger, J.L., 2001. Manual of applied field hydrogeology. McGraw-Hill, New York, 608 pp.